SUPPORTING INFORMATION

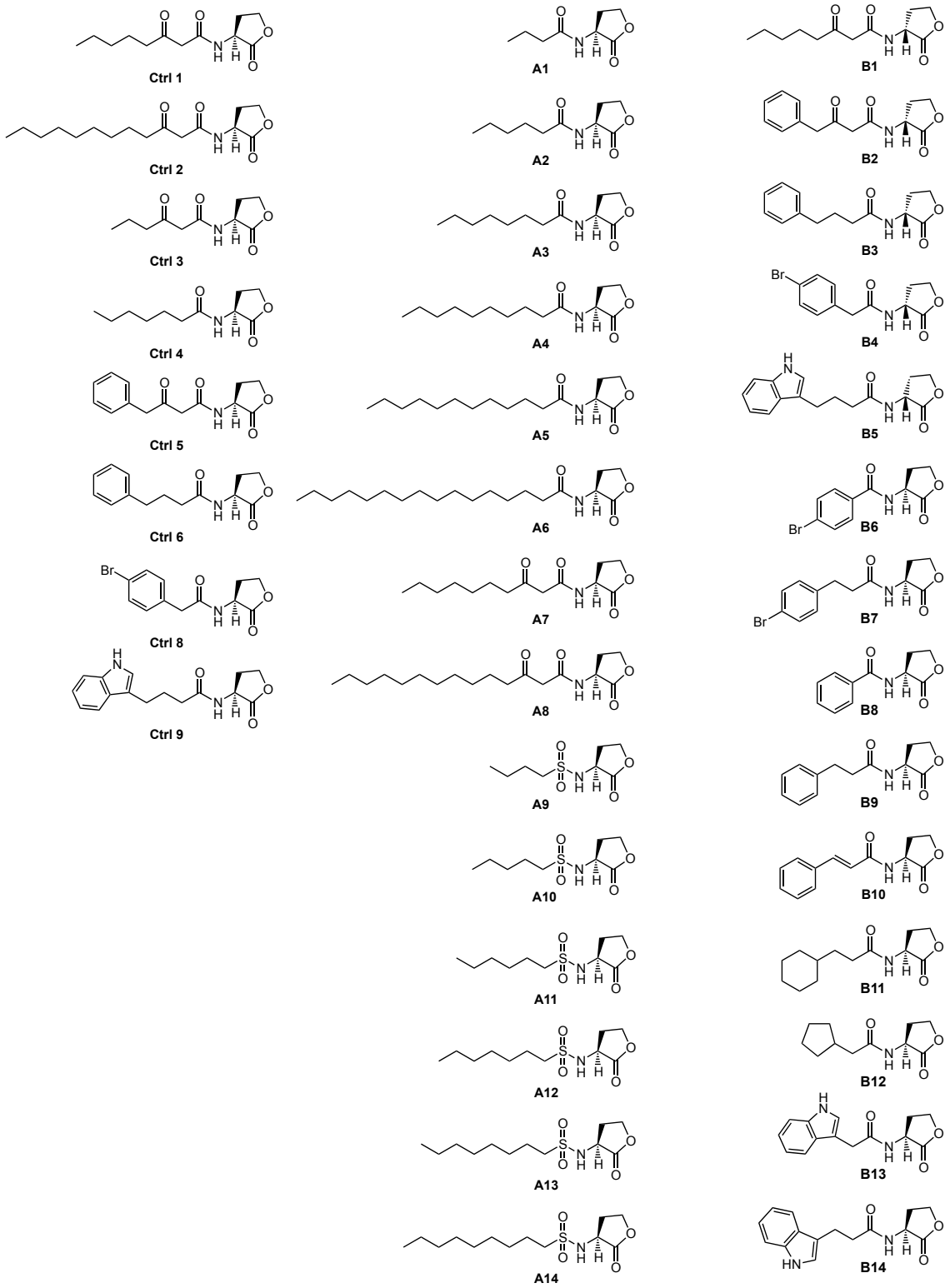

Figure S1. AHLs from the control, A, and B libraries examined in this study. Compound numbering is analogous to our earlier publications.[1]

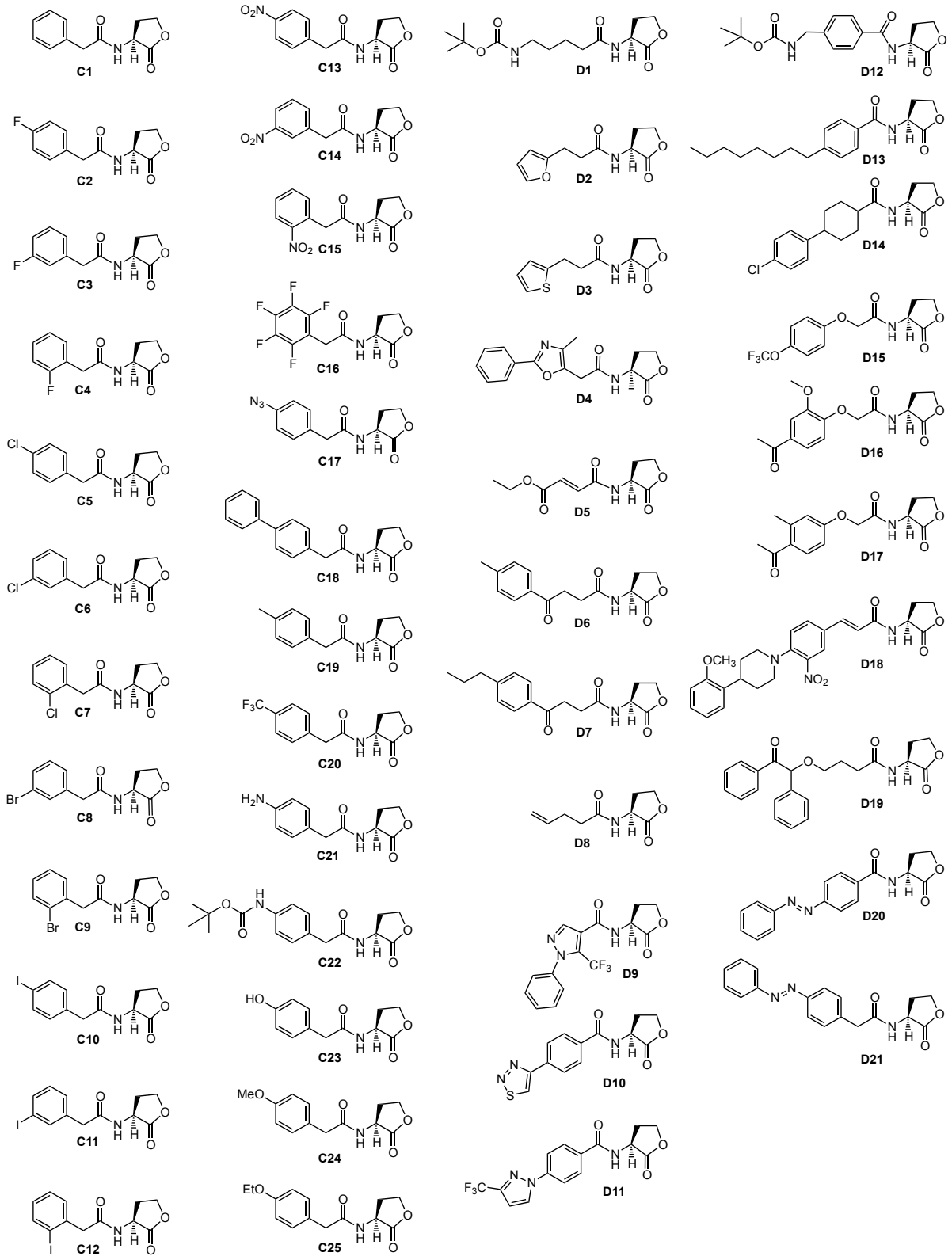

Figure S2. AHLs from the C and D libraries examined in this study. Compound numbering is analogous to our earlier publications.[1]

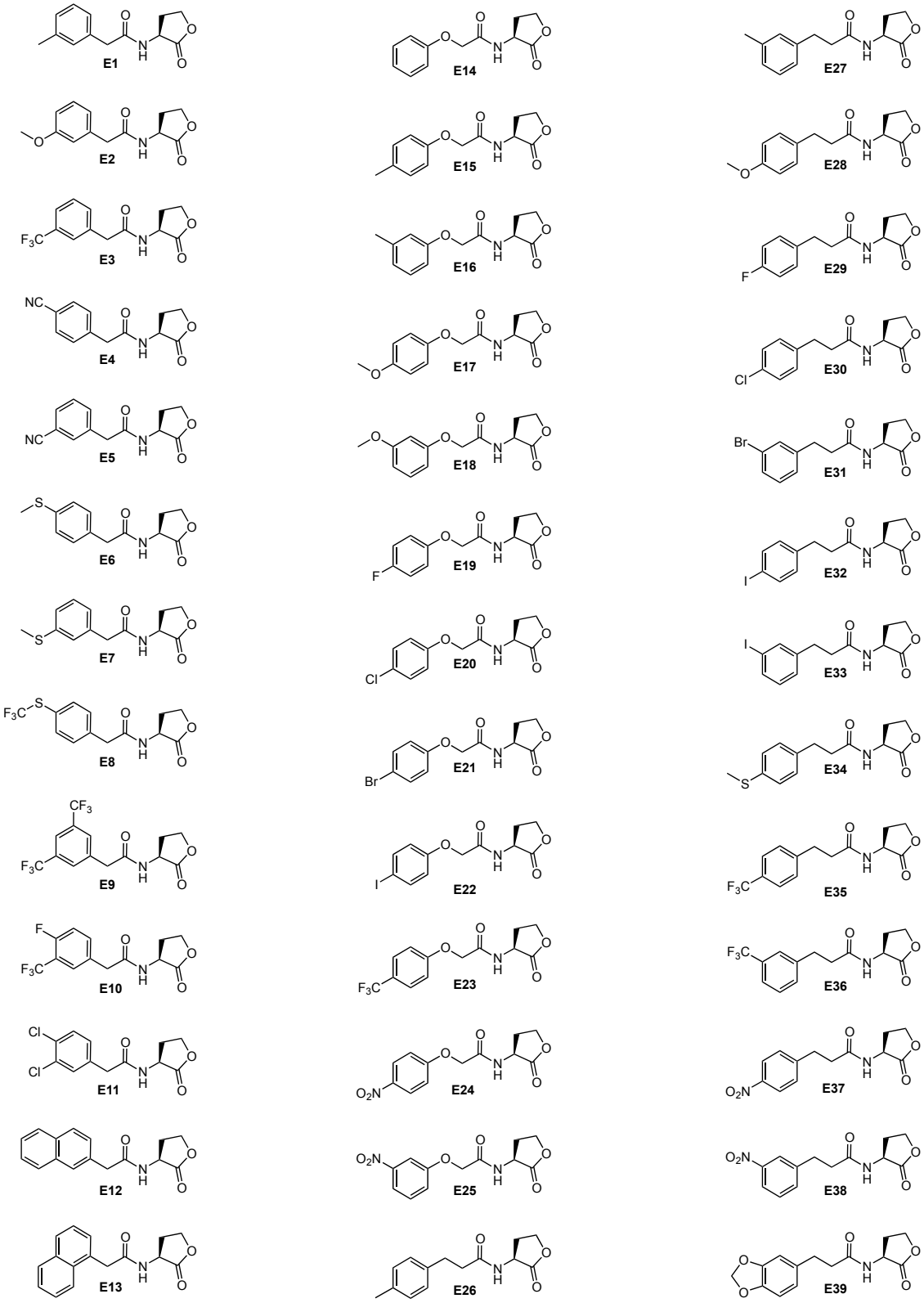

Figure S3. AHLs from the E library examined in this study. Compound numbering is analogous to our earlier publications.[2]

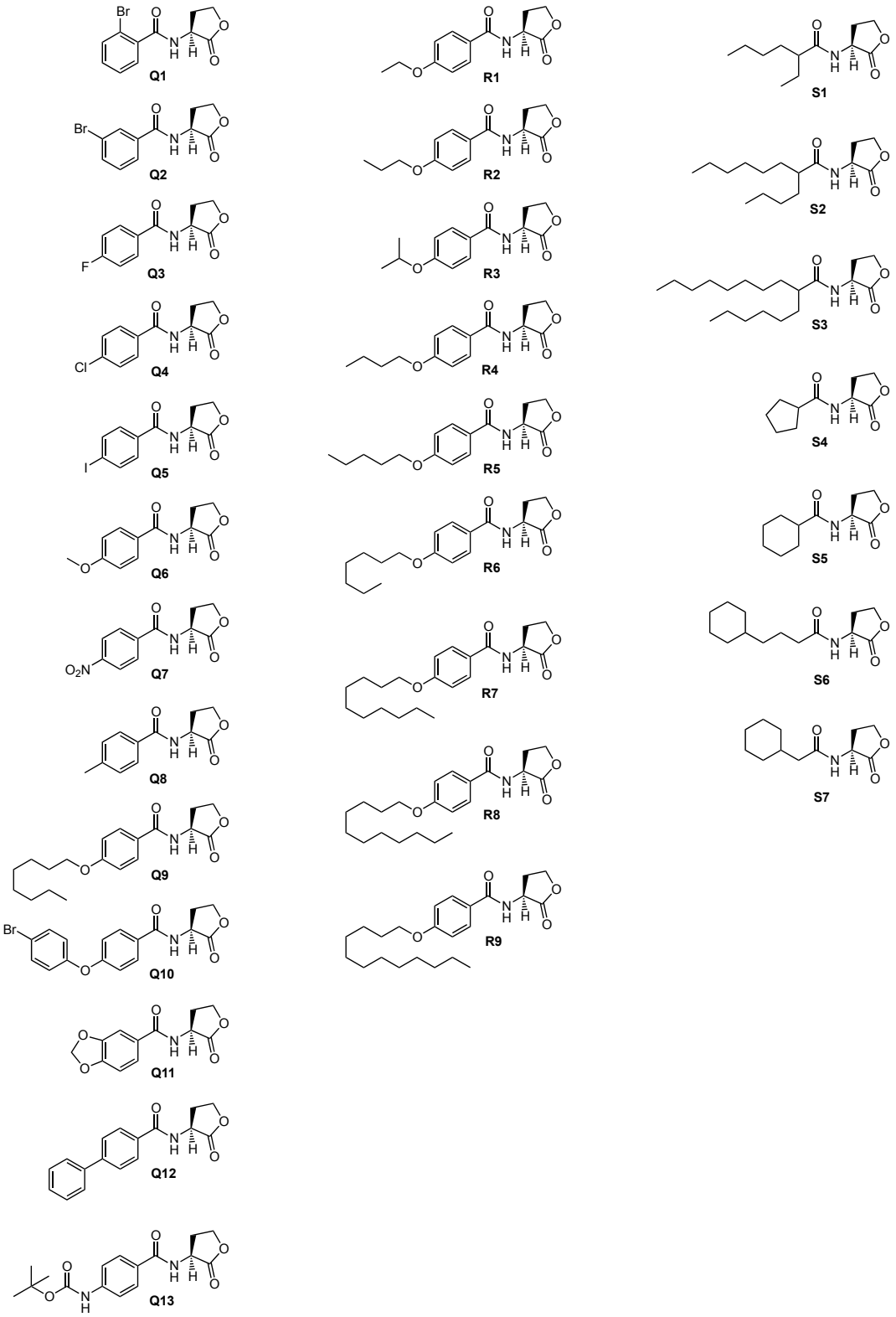

Figure S4. AHLs from the Q, R, and S libraries examined in this study. Compound numbering is analogous to our earlier publications.[3]

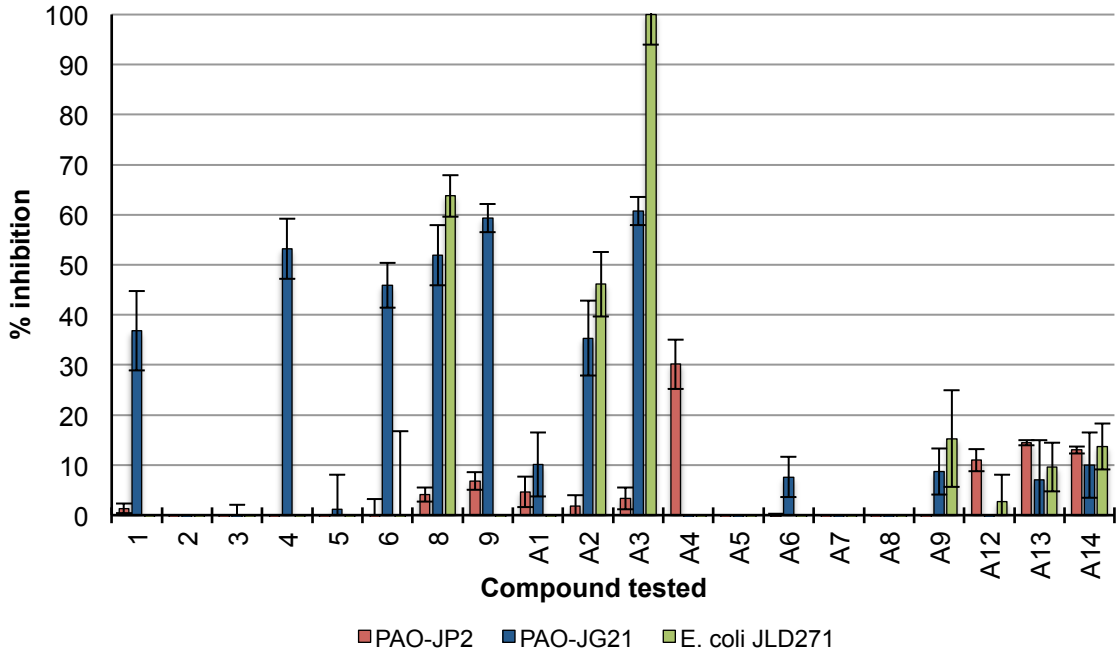

Figure S5. Primary LasR antagonism screening data for the control and A libraries in *P. aeruginosa* PAO-JP2 + p*lasI*LVAGFP, *P. aeruginosa* PAO-JG21 + p*lasI*LVAGFP, and *E. coli* JLD271 + pPROBE-KL. Antagonism assays were performed using the following compound concentrations and controls:

PAO-JP2: 10 μM of synthetic ligand against 100 nM OdDHL
Positive control (100 % inhibition) = 2 μL DMSO (no AHL added)
Negative control (0 % inhibition) = 100 nM OdDHL

PAO-JG21: 10 μM of synthetic ligand against 10 nM OdDHL
Positive control (100 % inhibition) = 2 μL DMSO (no AHL added)
Negative control (0 % inhibition) = 10 nM OdDHL

JLD271: 10 μM of synthetic ligand against 2 nM OdDHL
Positive control (100 % inhibition) = 2 μL DMSO (no AHL added)
Negative control (0 % inhibition) = 2 nM OdDHL

All fluorescence data were background-corrected by subtracting the negative control fluorescence value (wells containing reporter strain + 2 μL DMSO only) from the experimental value. Percent (%) LasR activity was measured by normalizing background-corrected value to fluorescence value obtained in wells containing reporter strain + OdDHL. Percent (%) LasR inhibition = 100% – % LasR activity.

All compounds were screened in triplicate over 3 separate trials. Error bars represent the SEM of 3 trials.

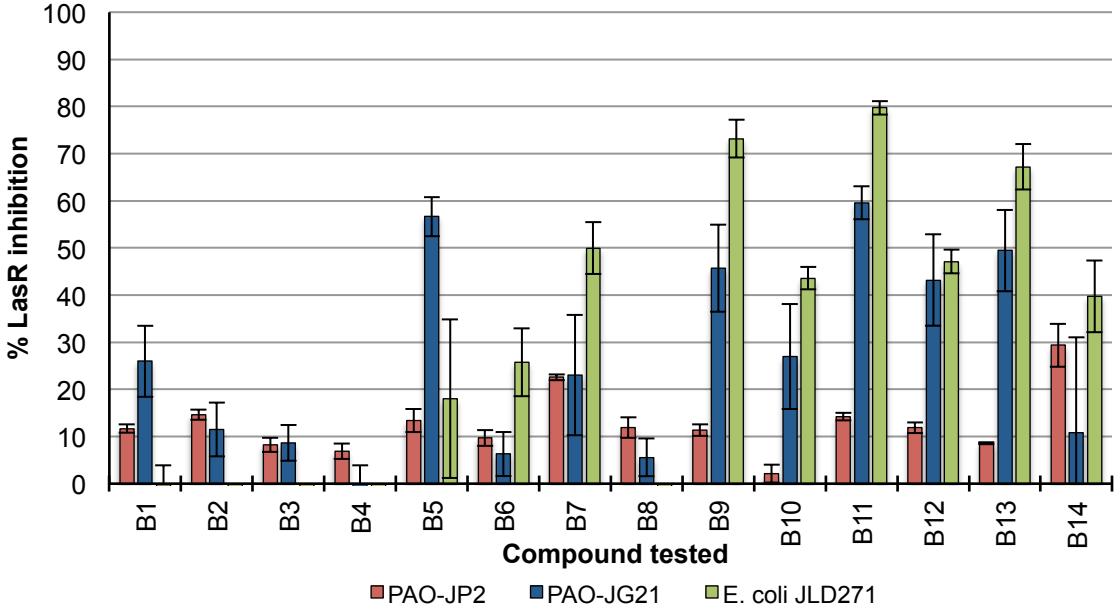

Figure S6. Primary LasR antagonism screening data for the B library in *P. aeruginosa* PAO-JP2 + p*lasI*LVAGFP, *P. aeruginosa* PAO-JG21 + p*lasI*LVAGFP, and *E. coli* JLD271 + pPROBE-KL. Antagonism assays were performed as described in Figure S5.

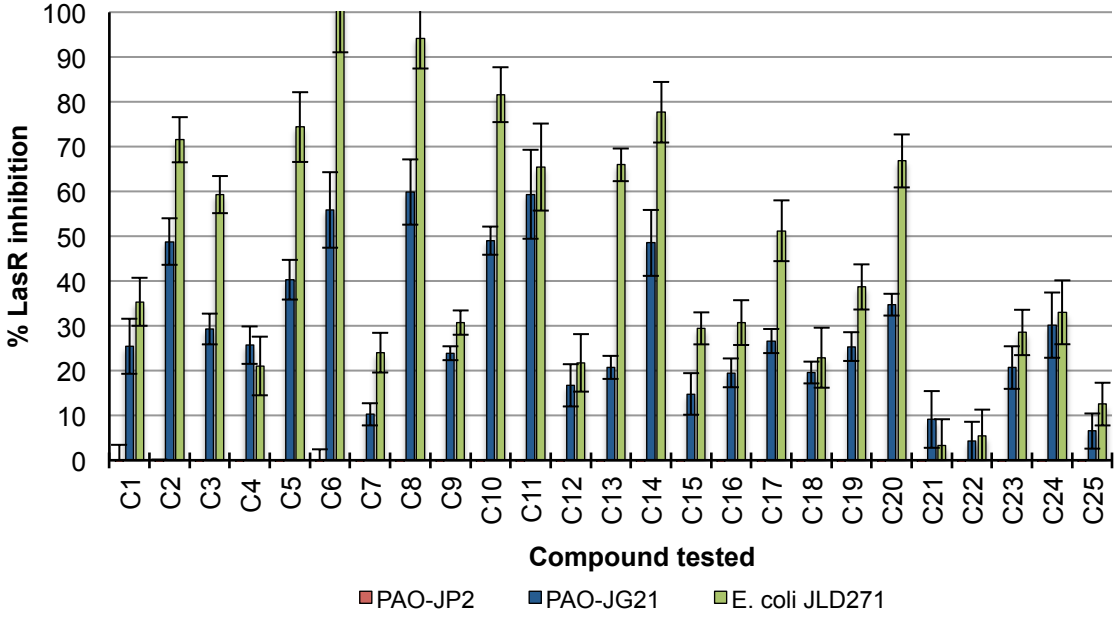

Figure S7. Primary LasR antagonism screening data for the C library in *P. aeruginosa* PAO-JP2 + p*lasI*LVAGFP, *P. aeruginosa* PAO-JG21 + p*lasI*LVAGFP, and *E. coli* JLD271 + pPROBE-KL. Antagonism assays were performed as described in Figure S5.

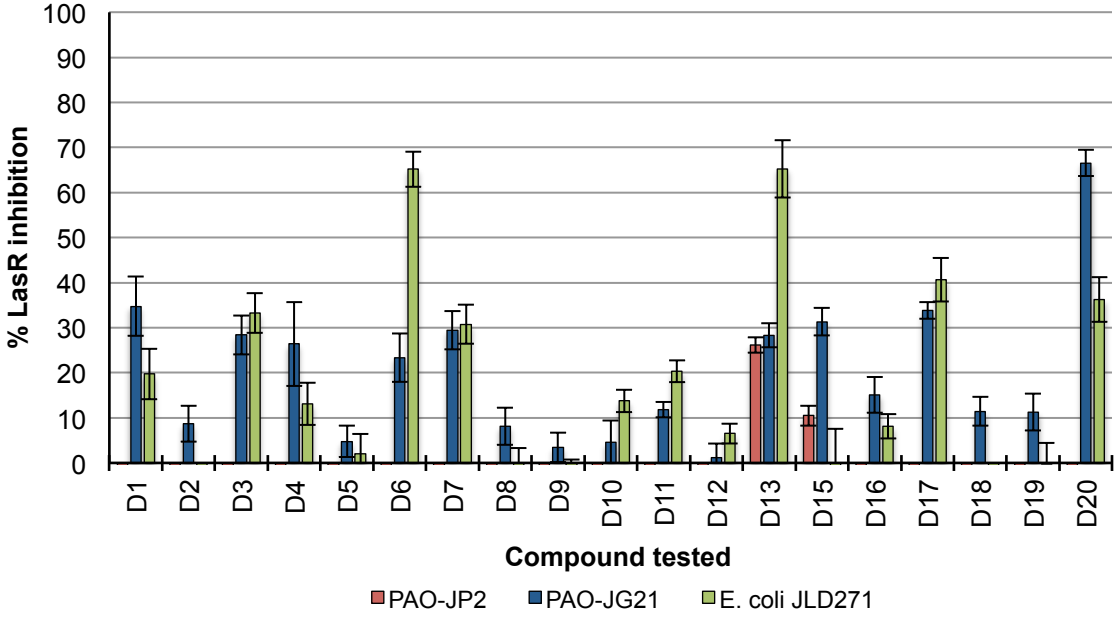

Figure S8. Primary LasR antagonism screening data for the D library in *P. aeruginosa* PAO-JP2 + p*lasI*LVAGFP, *P. aeruginosa* PAO-JG21 + p*lasI*LVAGFP, and *E. coli* JLD271 + pPROBE-KL. Antagonism assays were performed as described in Figure S5.

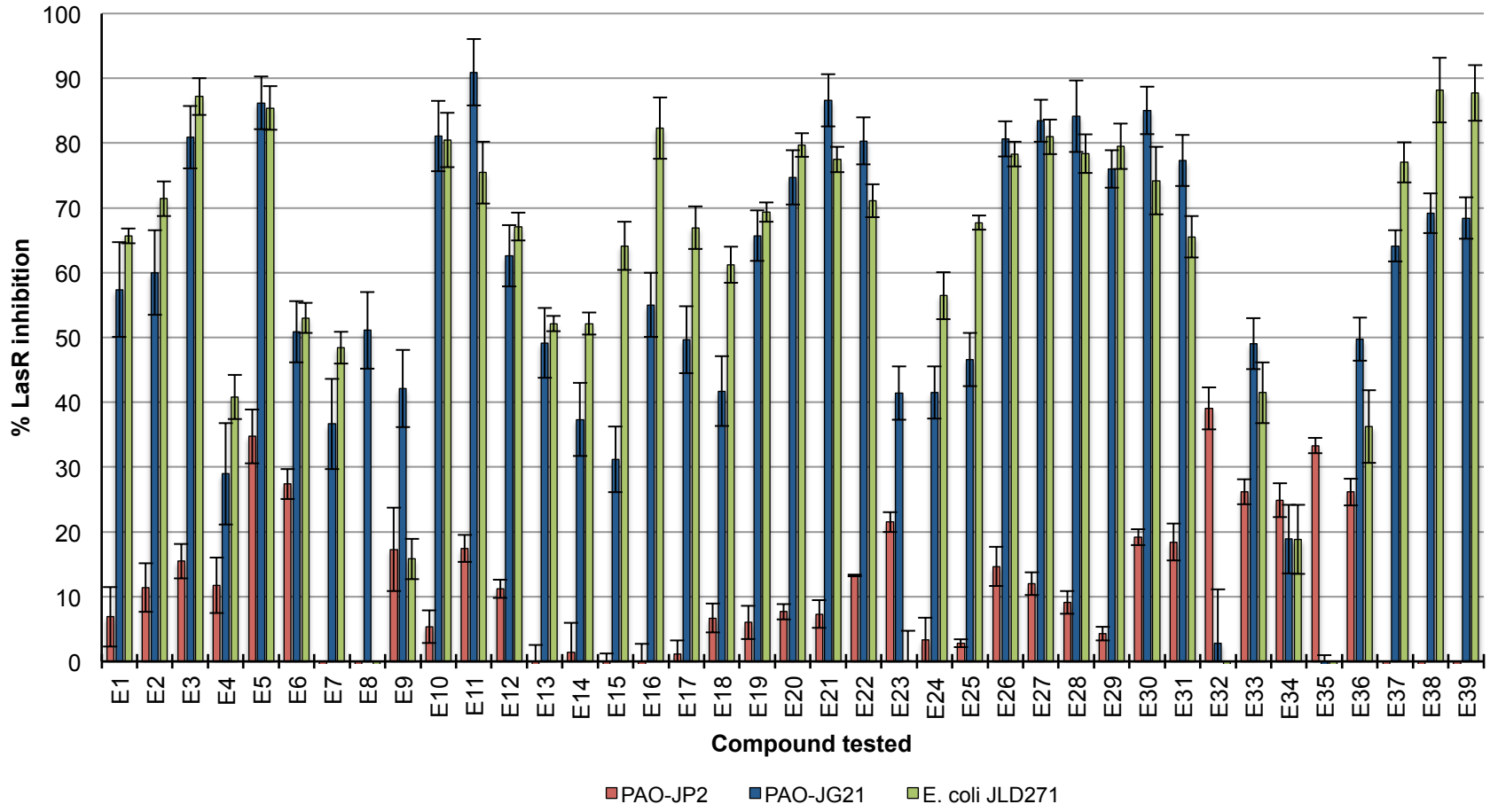

Figure S9. Primary LasR antagonism screening data for the E library in *P. aeruginosa* PAO-JP2 + p*lasI*LVAGFP, *P. aeruginosa* PAO-JG21 + p*lasI*LVAGFP, and *E. coli* JLD271 + pPROBE-KL. Antagonism assays were performed as described in Figure S5.

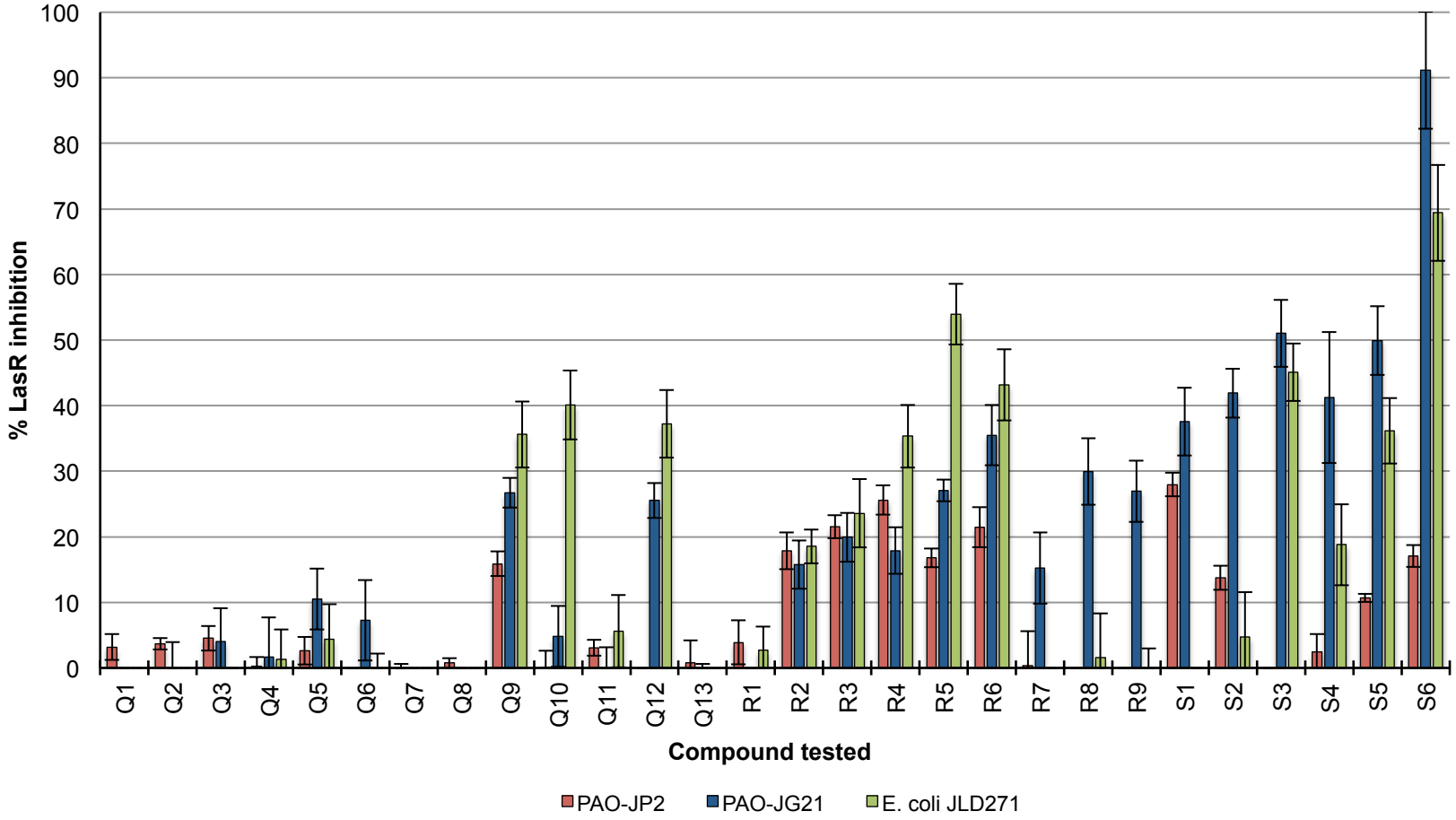

Figure S10. Primary LasR antagonism screening data for the Q, R, and S libraries in *P. aeruginosa* PAO-JP2 + p*lasI*LVAGFP, *P. aeruginosa* PAO-JG21 + p*lasI*LVAGFP, and *E. coli* JLD271 + pPROBE-KL. Antagonism assays were performed as described in Figure S5.

Table S1. List of the most active AHL-derived LasR antagonists identified in the *P. aeruginosa* PAO-JP2 (pump-active) GFP reporter screen and accompanying inhibition data. Primary data from plots in Figures S5–S10.

	Compound	LasR inhibition (%)
	A4	30
	B14	29
	D13	26[a]
	E5	35
≥ 25% inhibition	**E6**	27
	E32	39
	E33	26
	E35	33
	E36	26
	R4	25
	S1	28

[a] Compound displayed limited solubility at concentrations greater than 1 μM.

Table S2. List of the most active AHL-derived LasR antagonists identified in the *P. aeruginosa* PAO-JG21 (pump-mutant) GFP reporter screen and accompanying inhibition data. Primary data from plots in Figures S5–S10.

	Compound	LasR inhibition (%)
≥ 80% inhibition	**E3**	81
	E5	86
	E10	81
	E11	91
	E21	87
	E22	80
	E26	81
	E27	83
	E28	84
	E30	85
	S6	91

	Compound	LasR inhibition (%)	Compound	LasR inhibition (%)	Compound	LasR inhibition (%)
≥ 25% inhibition	**Ctrl 1**	37	**D1**	35	**E21**	87
	Ctrl 4	53	**D3**	28	**E22**	80
	Ctrl 6	46	**D4**	26	**E23**	41
	Ctrl 8	52	**D7**	29	**E24**	42
	Ctrl 9	59	**D13**	28[a]	**E25**	47
	A2	35	**D15**	31	**E26**	81
	A3	61	**D17**	34	**E27**	83
	B1	26	**D20**	67	**E28**	84
	B5	57	**E1**	57	**E29**	76
	B9	46	**E2**	60	**E30**	85
	B10	27	**E3**	81	**E31**	77
	B11	60	**E4**	29	**E33**	49
	B12	43	**E5**	86	**E36**	50
	B13	49	**E6**	51	**E37**	64
	C1	25	**E7**	37	**E38**	69
	C2	49	**E8**	51	**E39**	68
	C3	29	**E9**	42	**Q9**	27
	C4	26	**E10**	81	**Q12**	26
	C5	40	**E11**	91	**R5**	27
	C6	56	**E12**	63	**R6**	35
	C8	60	**E13**	49	**R8**	30
	C10	49	**E14**	37	**R9**	27
	C11	59	**E15**	31	**S1**	38
	C14	30	**E16**	55	**S2**	42
	C17	35	**E17**	50	**S3**	51
	C19	25	**E18**	42	**S4**	41
	C20	35	**E19**	66	**S5**	50
	C24	30	**E20**	75	**S6**	91

[a] Compound displayed limited solubility at concentrations greater than 1 μM.

Table S3. List of the most active AHL-derived LasR antagonists identified in the *E. coli* JLD271 GFP reporter screen and accompanying inhibition data. Primary data from plots in Figures S5–S10.

	Compound	LasR inhibition (%)
≥ 80% inhibition	**A3**	99
	B11	80
	C6	100
	C8	94
	C10	82
	E3	87
	E5	85
	E10	80
	E16	82
	E20	80
	E27	81
	E38	88
	E39	88

	Compound	LasR inhibition (%)	Compound	LasR inhibition (%)	Compound	LasR inhibition (%)
≥ 25% inhibition	**Ctrl 8**	64	**C20**	67	**E20**	80
	A2	46	**C23**	29	**E21**	77
	A3	99	**C24**	33	**E22**	71
	B6	26	**D3**	33	**E24**	56
	B7	50	**D6**	65	**E25**	68
	B9	73	**D7**	31	**E26**	78
	B10	44	**D13**	65[a]	**E27**	81
	B11	80	**D17**	41	**E28**	78
	B12	47	**D20**	36	**E29**	79
	B13	67	**E1**	66	**E30**	74
	B14	40	**E2**	71	**E31**	66
	C1	35	**E3**	87	**E33**	41
	C2	72	**E4**	41	**E36**	36
	C3	59	**E5**	85	**E37**	77
	C5	74	**E6**	53	**E38**	88
	C6	100	**E7**	48	**E39**	88
	C8	94	**E10**	80	**Q9**	36
	C9	31	**E11**	75	**Q10**	40
	C10	82	**E12**	67	**Q12**	37
	C11	65	**E13**	52	**R4**	35
	C13	66	**E14**	52	**R5**	54
	C14	78	**E15**	64	**R6**	43
	C15	29	**E16**	82	**S3**	45
	C16	31	**E17**	67	**S5**	36
	C17	51	**E18**	61	**S6**	69
	C19	39	**E19**	69		

[a] Compound displayed limited solubility at concentrations greater than 1 μM.

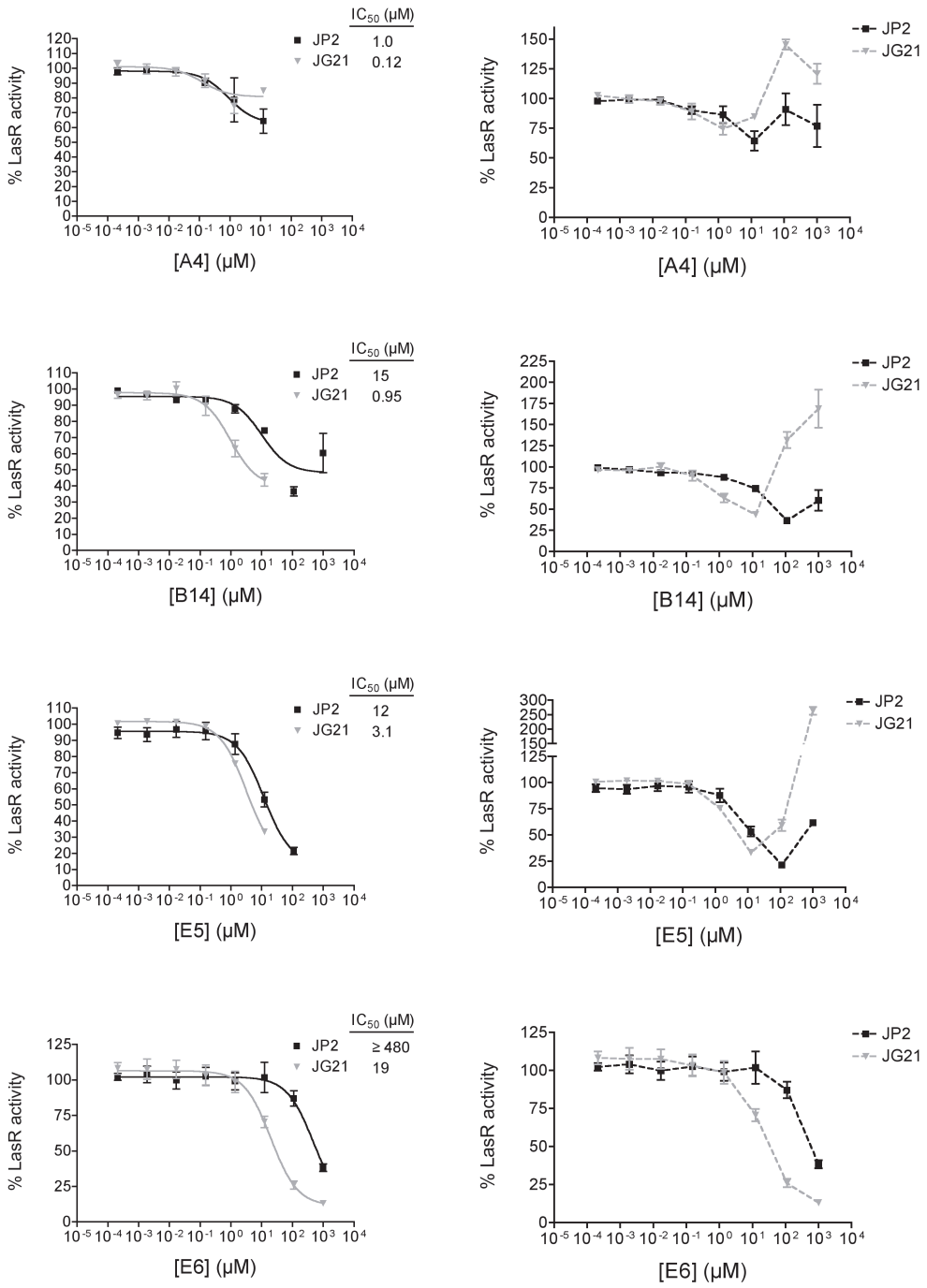

Figure S11. LasR antagonism dose responses and IC_{50} values for AHLs **A4**, **B14**, **E5**, and **E6** in *P. aeruginosa* PAO-JP2 and PAO-JG21. Plots on the left are truncated to show the dose response curves of the compounds in the inhibitory concentration range for each strain. Plots on the right show the full dose response including non-monotonic behavior, if applicable. Synthetic compounds were screened against 100 nM and 10 nM OdDHL in PAO-JP2 and PAO-JG21, respectively, over varying concentrations. IC_{50} values were calculated from the truncated plots using GraphPad Prism. Error bars, SEM of n = 3 trials.

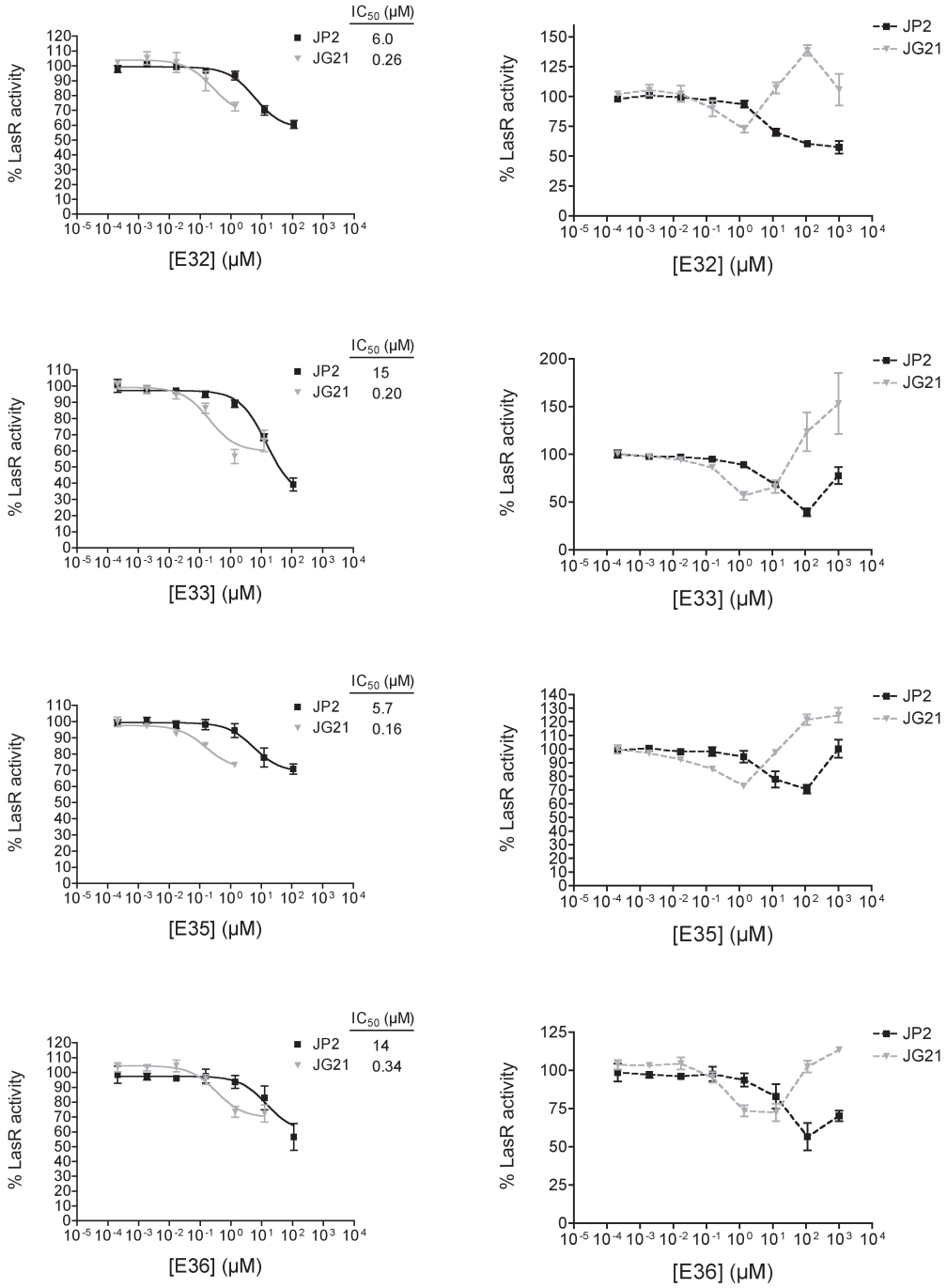

Figure S12. LasR antagonism dose responses and IC_{50} values for AHLs **E32**, **E33**, **E35**, and **E36** in *P. aeruginosa* PAO-JP2 and PAO-JG21. Plots on the left are truncated to show the dose response curves of the compounds in the inhibitory concentration range for each strain. Plots on the right show the full dose response including non-monotonic behavior, if applicable. Synthetic compounds were screened against 100 nM and 10 nM OdDHL in PAO-JP2 and PAO-JG21, respectively, over varying concentrations. IC_{50} values were calculated from the truncated plots using GraphPad Prism. Error bars, SEM of n = 3 trials.

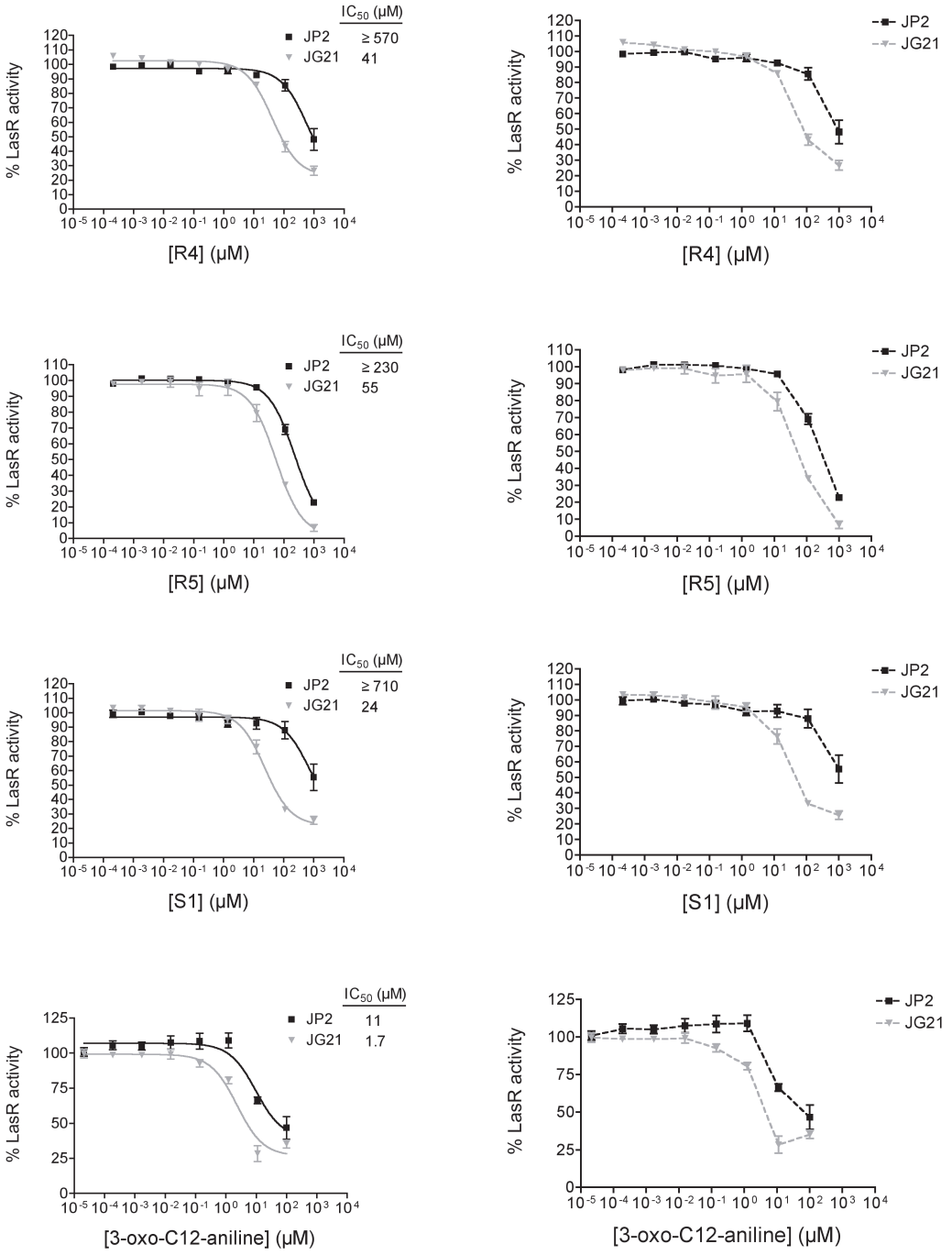

Figure S13. LasR antagonism dose responses and IC_{50} values for AHLs **R4**, **R5**, **S1**, and 3-oxo-C12-aniline in *P. aeruginosa* PAO-JP2 and PAO-JG21. Plots on the left are truncated to show the dose response curves of the compounds in the inhibitory concentration range for each strain. Plots on the right show the full dose response including non-monotonic behavior, if applicable. Synthetic ligands screened against 100 nM and 10 nM OdDHL in PAO-JP2 and PAO-JG21, respectively, over varying concentrations of inhibitor. IC_{50} values were calculated from the truncated plots using GraphPad Prism. Error bars, SEM of n = 3 trials.

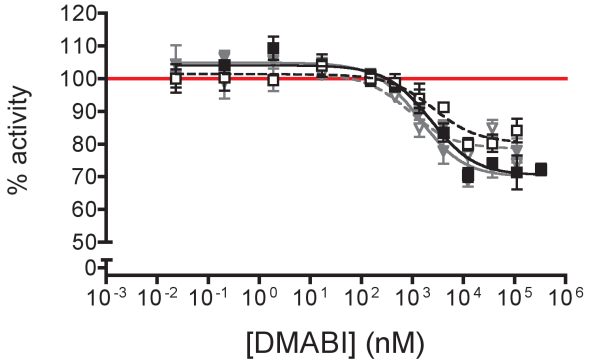

Trial	IC_{50} (μM)
PAO-JP2	2.3
PAO-JP2 + 25 μg/mL PAßN	2.9
PAO-JG21	1.4
PAO-JG21 + 25 μg/mL PAßN	0.89

Figure S14. LasR antagonism dose response curves for DMABI in *P. aeruginosa* PAO-JP2 and PAO-JG21 in the absence and presence of PAßN. DMABI potency was not affected by removal of MexAB-OprM or addition of the RND pump inhibitor PAßN. Antagonism assays were performed using the following compound concentrations and controls:

PAO-JP2:
Variable concentrations of DMABI against 100 nM OdDHL
Positive control (100 % inhibition) = 2 μL DMSO (no AHL added)
Negative control (0 % inhibition; red line) = 100 nM OdDHL

PAO-JG21; PAO-JP2 + PAßN; PAO-JG21 + PAßN:
Variable concentrations of DMABI against 10 nM OdDHL
Positive control (100 % inhibition) = 2 μL DMSO (no AHL added)
Negative control (0 % inhibition; red line) = 10 nM OdDHL

All fluorescence data were background-corrected by subtracting the negative control fluorescence value (wells containing reporter strain + 2 μL DMSO only) from the experimental value. Percent (%) LasR activity was measured by normalizing the background-corrected value to the fluorescence value obtained in wells containing reporter strain + OdDHL. Percent (%) LasR inhibition = 100% – % LasR activity.

IC_{50} values were calculated using GraphPad Prism. Error bars, SEM of n = 3 trials.

The % activity scale on the y-axis has been zoomed to show that LasR inhibition by DMABI, while modest, is significant relative to the negative control.

References.

[1] G. D. Geske, J. C. O'Neill, D. M. Miller, M. E. Mattmann, H. E. Blackwell, *J. Am. Chem. Soc.* **2007**, *129*, 13613-13625.

[2] G. D. Geske, M. E. Mattmann, H. E. Blackwell, *Bioorg. Med. Chem. Lett.* **2008**, *18*, 5978-5981.

[3] M. E. Mattmann, P. M. Shipway, N. J. Heth, H. E. Blackwell, *ChemBioChem* **2011**, *12*, 942-949.